

## Van der Waals forces between heavy alkali atoms and gold surfaces: Comparison of measured and predicted values

A. Shih\*

*Surface Chemistry Section, National Bureau of Standards, Washington, D.C. 20234*

V. A. Parsegian

*Physical Sciences Laboratory, Division of Computer Research and Technology, National Institutes of Health, Bethesda, Maryland 20014*

(Received 4 December 1974; revised manuscript received 27 May 1975)

The Van der Waals potentials between heavy alkali-metal atoms (Cs, Rb, K) and gold surfaces have been investigated by the atomic-beam-deflection technique. The result is consistent with a potential of the form  $V(R) = -k/R^3$ . The observed interaction constant  $k$  is  $7.0 \pm 0.29 D^2$ ,  $6.04 \pm 0.30 D^2$ , and  $5.10 \pm 0.62 D^2$  for Cs, Rb, and K, respectively. These values are smaller than the predictions based on all available theories. At best there is agreement within 60% for estimates based on the macroscopic continuum theory of Lifshitz. Other models disagree with measurements by factors of three (200% difference) or more.

### INTRODUCTION

The potential energy  $V(R)$  of an atom or a molecule at a distance  $R$  from a conducting surface has been the subject of many theoretical studies. Lennard-Jones,<sup>1</sup> Bardeen,<sup>2</sup> and Margenau and Pollard<sup>3</sup> have derived a potential of an  $R^{-3}$  form. Casimir and Polder,<sup>4</sup> Mavroyannis,<sup>5</sup> McLachlan,<sup>6</sup> Boyer,<sup>7</sup> and Parsegian<sup>8</sup> obtain this result at small distances where electromagnetic retardation is not important; they also find the large-separation asymptotic form of the potential to be  $R^{-4}$ . Contrary to the above theories, Prosen and Sachs<sup>9</sup> derive a potential of the form  $R^{-2} \ln(2k_F R)$  where  $k_F$  is the magnitude of the Fermi wave vector.

Experimental investigations of this potential have been found to be possible by measuring the deflection of an atomic beam passing near a cylindrical surface.<sup>10,11</sup> So far, this method can detect the potential over a range of impact parameters from  $\sim 300$  to  $\sim 800$  Å.

Shih, Raskin, and Kusch<sup>10</sup> detected the attraction between polar molecules (CsCl, CsF) and a stainless-steel cylinder; Shih<sup>11</sup> studied that between a Cs atom and a gold surface. Those results were shown to be inconsistent with an  $R^{-2}$  potential, but they were insufficient to allow a clear distinction between an  $R^{-3}$  and an  $R^{-4}$  power law. Preference for the  $R^{-3}$  was based solely on the ground that that form enjoyed a stronger theoretical basis.

Finer discrimination has been found in the present work. The same apparatus is employed, but more extensive measurements were made with an atomic cesium beam. These data, together with those from beams of rubidium and potassium, were subjected to statistical analysis by a  $\chi^2$  test. Using this standard "goodness of fit" curve-fitting criterion, it is found that an  $R^{-3}$  potential is clear-

ly preferred to  $R^{-4}$  or  $R^{-2}$ .

Also, beam and substrate materials were chosen for which predictions could be made using available theories. In no case is there perfect agreement with observation. Computations based on the work of Lennard-Jones,<sup>1</sup> Bardeen,<sup>2</sup> and Mavroyannis<sup>5</sup> are greater than experiment by factors of three to four. Predictions using the formula of Parsegian<sup>8</sup> based on the Lifshitz<sup>12</sup> theory are greater by about 60%. Possible reasons for the remaining discrepancy—surface contamination, surface roughness, or theoretical assumptions—are considered.

### EXPERIMENT AND RESULTS

A beam of neutral atoms evaporated from a molecular beam oven is further defined by passage through a narrow slit (Fig. 1). Because the oven slit is wide ( $\sim 0.01$  cm) relative to the  $10\text{-}\mu\text{m}$  ( $0.001$  cm) defining slit, the beam diverges from the  $10\text{-}\mu\text{m}$  slit. This divergent beam is partially intercepted by a fixed cylindrical surface. We measure the beam intensity "profile"  $I(S)$  relative to the full beam intensity  $I_0$  as a function of deflection distance  $S$  into the geometric shadow of the surface.

The detection of neutral atoms is by the surface ionization of the atoms on a movable, hot W filament.

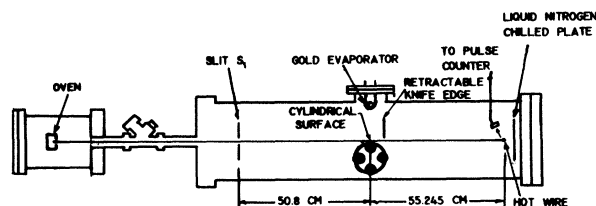


FIG. 1. Atomic beam apparatus.

Among the atoms, only Cs, Rb, and K can be detected efficiently this way, and thus this work covers only these three atomic species.

The alkali-metal beams are produced from the evaporation of high-purity alkali metals; the purities are 99.98%, 99%, and 99.95% for Cs, Rb, and K, respectively.

The apparatus (see Fig. 1) is housed inside an ultrahigh-vacuum system, and measurements are taken with the pressure below  $5 \times 10^{-11}$  Torr.

The observed beam profile is to be compared to a family of profiles calculated on the basis of the inverse second-, third-, fourth-power potential. The comparison will determine whether or not, within experimental limitation, the interaction can be described through one of these potentials.

We have used the conventional  $\chi^2$  test for the statistical method to test the "goodness" of a curve fitting.<sup>13,14</sup> Tables I, II, and III summarize our application of this test to each of the five runs made on K, Rb, and Cs beams. In the tables are listed the  $\chi^2$  values ( $Q$ ) and the corresponding probabilities  $P$  of measured deviations occurring larger than those observed (under the assumption that the theoretical form being tested is correct). With one possible exception (the third Cs run), the potential form  $V = -k/R^3$  is strongly favored over  $R^{-2}$  and  $R^{-4}$  dependences. This test indicates further that the  $R^{-3}$  potential is acceptable, while the  $R^{-2}$  or  $R^{-4}$  potential is not.

In Fig. 2, we have plotted the deviations of measured intensity  $Y(S)$  from predicted intensity  $I(S)$  in units of standard deviation  $\delta(S)$ ,  $[Y(S) - I(S)]/\delta(S)$ , as a function of deflection  $S$ , for three different forms of the interaction potential; the values of  $Y(S)$  are appropriate to one data run for the system Rb/Au. It is unambiguous that the deviation of the measured intensity  $Y(S)$  for either an  $R^{-2}$  or  $R^{-4}$  potential is systematic, as well as large. By contrast,  $Y(S)$  seldom differs by more than  $\pm \delta(S)$  from  $I(S)$  based on an  $R^{-3}$  potential. Note also that the distinction between  $R^{-4}$  and  $R^{-3}$  potentials is more apparent at small deviations.

TABLE I. Probability  $P$  of fit to  $V = -kR^{-n}$  for potassium over gold.  $Q$  is the  $\chi^2$  value for each set of points. Values of  $Q$  greater than 30 imply probabilities of less than 1%. Typically,  $P \leq 5\%$  is the criterion for poor fit.

Run no.	$R^{-2}$		$R^{-3}$		$R^{-4}$	
	$P$	( $Q$ )	$P$	( $Q$ )	$P$	( $Q$ )
1		(71.1)	5.3%	(23.5)		(102)
2		(72.5)	41%	(14.5)		(79)
3		(67.9)	95%	(6.69)		(76.7)
4		(88.9)	30%	(16.2)		(82)

TABLE II. Probability  $P$  of fit to  $V = -kR^{-n}$  for rubidium over gold.  $Q$  is the  $\chi^2$  value for each set of points. Values of  $Q$  greater than 30 imply probabilities of less than 1%.

Run no.	$R^{-2}$		$R^{-3}$		$R^{-4}$	
	$P$	( $Q$ )	$P$	( $Q$ )	$P$	( $Q$ )
1		(147)	5.8%	(23.1)		(126)
2		(155)	92%	(7.3)		(52.5)
3		(175)	46%	(13.9)		(48.9)
4		(249)	9.7%	(21.2)	3.3%	(25.2)
5		(197)	64%	(11.6)		(33.8)

For this reason, further measurement at greater deflections would not help to discriminate between  $R^{-3}$  and  $R^{-4}$  attraction energies.

We now use the data to extract the interaction constants  $k$  appearing in the form  $V = -k/R^3$ . These are obtained (Table IV) through a least-squares fit for each of the five Cs or Rb runs and the four K runs. An average  $\bar{k}$  and standard deviation  $\delta$  are then derived from the sum of individual runs. For five runs the error  $\Delta k = 1.3\delta$ ; for four,  $\Delta k = 1.6\delta$ , where the range  $\bar{k} + \Delta k$  represents the interval with 95% confidence level.<sup>15</sup>

The observed beam profiles are shown in Figs. 3 and 4; at each  $S$  the average of the five measurements is shown, and the error bars indicate one standard deviation for these five measurements. Also shown in the figures are the theoretical profiles calculated based on the potential  $-k/R^3$ .

#### THEORETICAL PREDICTIONS

With the exception of Prosen and Sach's model,<sup>9</sup> all other theories predict an  $R^{-3}$  potential where the retardation effect is unimportant. This is an agreement with our data. We now evaluate the interaction constants predicted by these theories and compare them to the observed values.

In the Lennard-Jones model,<sup>1</sup> the surface is assumed to be an ideal conductor. For a spherically symmetric atom such as alkali atoms, the Lennard-Jones interaction constant is

TABLE III. Probability of fit to  $V = -kR^{-n}$  for Cs over gold.  $Q$  is the  $\chi^2$  value for each set of points. Values of  $Q$  greater than 30 imply probabilities of less than 1%.

Run no.	$R^{-2}$		$R^{-3}$		$R^{-4}$	
	$P$	( $Q$ )	$P$	( $Q$ )	$P$	( $Q$ )
1		(133)	12.7%	(20.1)		(53.7)
2		(142)	43.5%	(14.2)		(33.8)
3		(193)	1.90%	(27.0)	2.8%	(25.7)
4		(162)	22.1%	(17.7)	3.8%	(24.7)
5		(141)	37.8%	(15.0)		(38.6)

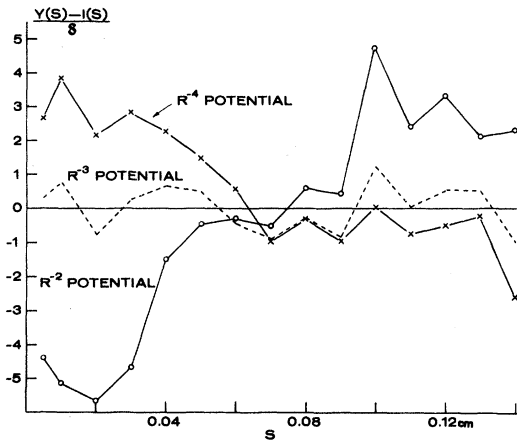


FIG. 2. Deviation  $Y(S) - I(S)$  evaluated in units of  $\delta(S)$  is plotted as a function of deflection  $S$ . The values of  $Y(S)$  are appropriate to one data run for the system Rb/Au; the values of  $I(S)$  are the least-squares-adjusted theoretical values based on  $R^{-2}$ ,  $R^{-3}$ , and  $R^{-4}$  potentials.

$$k_{L-J} = -\frac{e^2}{16} \left( \frac{4}{3} \sum_i \langle i | r^2 | i \rangle - \sum_{i \neq j} [ |\langle i | x | j \rangle|^2 + |\langle i | y | j \rangle|^2 + 2|\langle i | z | j \rangle|^2 ] \dots \right), \quad (1)$$

where  $i$  and  $j$  label the electronic orbitals in the atom. For accuracy, we have retained the second term which is usually found to be negligibly small by Lennard-Jones but significant here for heavy alkali atoms (see Table V).

We have evaluated Eq. (1) using the Hartree-Fock wave function of Froese Fischer,<sup>16</sup> and the result is summarized in Table V.  $k_{L-J}$  is the upper limit for the Van der Waals interaction constant, since an ideally conducting surface is assumed. The  $k_{L-J}$  evaluated are larger than the observed values by factors of 5.57, 4.91, and 4.49, respectively, for Cs, Rb, and K.

TABLE IV. Interaction constants fitting the form  $V = -k/R^3$  for the potential in Debye units ( $D^2 = 10^{-36}$  erg  $\text{cm}^3$ ). Error range  $\Delta k$  is  $1.3\delta$  for Cs and Rb, and  $1.6\delta$  for K, representing 95% confidence limits.

Run no.	$k$ (Cs) ( $D^2$ )	$k$ (Rb) ( $D^2$ )	$k$ (K) ( $D^2$ )
1	7.14	6.02	4.65
2	7.15	5.8	5.02
3	6.76	5.95	5.09
4	6.75	6.41	5.62
5	7.16	6.02	
Average $\bar{k} \pm \Delta k$	$6.97 \pm 0.29$	$6.04 \pm 0.30$	$5.10 \pm 0.62$
Standard deviation $\delta$	0.20	0.23	0.39

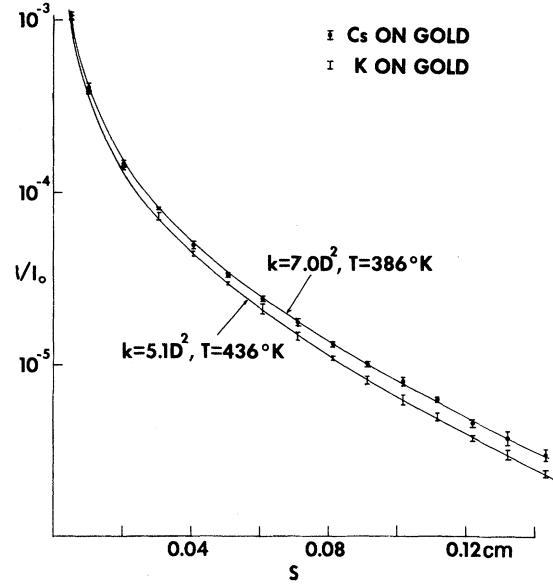


FIG. 3. Observed profiles of a Cs and a K beam on a gold surface together with the respective theoretical profiles based on  $R^{-3}$  potentials.

The finite conductivity of the metal surface is included by Bardeen<sup>2</sup> and Mavroyannis.<sup>5</sup> The Bardeen interaction constant is

$$k_B = k_{L-J} \frac{Ce^2/2r_s\Delta}{1 + Ce^2/2r_s\Delta}, \quad (2)$$

and the Mavroyannis interaction constant is

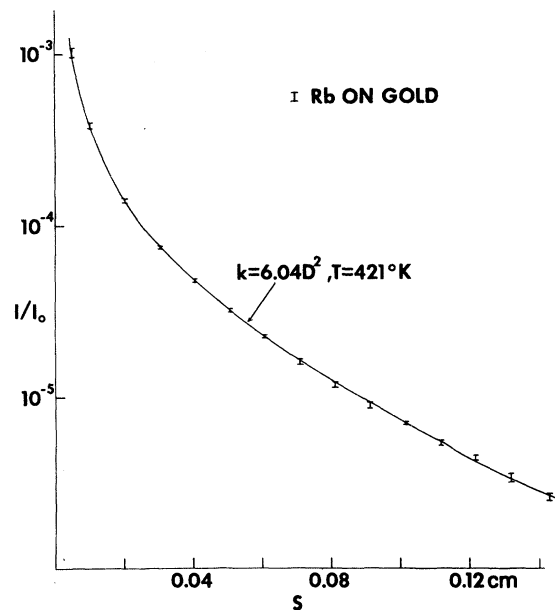


FIG. 4. Observed profiles of a Rb beam on a gold surface together with theoretical profiles based on an  $R^{-3}$  potential.

TABLE V. Computation of interaction constant  $k_{L-J}$  Eq. (1) ( $D^2 = 10^{-36}$  erg cm<sup>3</sup>).

	$\frac{4}{3} \sum_i \langle i   r^2   i \rangle$ (a.u.)	$\sum_{i \neq j}  \langle i   x   j \rangle ^2 +  \langle i   y   j \rangle ^2 + 2  \langle i   z   j \rangle ^2$ (a.u.)	Interaction constant $k_{L-J}$ ( $D^2$ )
Cs	130.0	31.1	40.1
Rb	91.0	18.2	29.4
K	68.3	10.8	23.2

$$k_M = k_{L-J} \frac{\hbar \omega_p / \sqrt{2}}{(8k_{L-J} / \alpha) + \hbar \omega_p / \sqrt{2}}. \quad (3)$$

Here  $C$  is 2.6 for monovalent metals, and  $r_s$  is the radius of a spherical volume of space occupied by a conducting electron,  $\Delta$  is the ionization potential of the atom,  $\omega_p$  is the plasma frequency of the metal, and  $\alpha$  is the static polarizability of the atom.

For gold,  $\hbar \omega_p = 9$  eV.<sup>17</sup> From this plasma frequency, we obtain a value of  $r_s = 1.6$  Å.  $\Delta$  is 3.89, 4.18, and 4.34 eV<sup>18</sup>;  $\alpha$  is 59.6, 47.5, and 43.7 Å<sup>3</sup>, for Cs, Rb, and K, respectively.<sup>19</sup> Calculated values of  $k_B$  and  $k_M$  are listed in Table VI. These values are still substantially larger than our observations.

The accuracy of the  $k_{L-J}$ ,  $k_B$ , or  $k_M$  evaluation depends, of course, on the accuracy of the atomic wave functions used. All we know about the accuracy of Hartree-Fock wave functions is that they are at least very consistent with each other as far as the calculation of Eq. (1) is concerned. We have also evaluated  $k_{L-J}$  for K, using the wave function of Clementi.<sup>20</sup> This result agrees well with the value obtained using the wave function of Froese Fischer (cf. Table VII). However, this agreement does not necessarily imply the accuracy of the wave functions themselves. (In an earlier paper,<sup>11</sup> these theoretical constants were found using Boyer's approximation, which depends only on the experimentally observable quantities, but which is good only for atoms with two levels. Those results, although smaller than the one calculated here, were also substantially larger than

the observed values. Therefore, there is no ambiguity as to whether the discrepancy is indeed real.) For the theoretical values for  $k_{L-J}$ ,  $k_B$ , or  $k_M$ , we nevertheless adopted the Hartree-Fock wave functions because these are the best available.

In the theories of Casimir and Polder,<sup>4</sup> McLachlan,<sup>6</sup> and Boyer,<sup>7</sup> an ideal conductor is assumed. Thus in the nonretarded limit, these are equivalent to the Lennard-Jones potential. Margenau and Pollard<sup>3</sup> have calculated the energy for an atom whose dominant transition energy  $\Delta$  is greater than the energies of the principal absorption bands of the metal, as in the case of light inert gases with most good conductors. For a beam of alkali-metal atoms deflected by a gold surface, the condition of Margenau and Pollard is not satisfied.

The interaction potential derived by Parsegian<sup>8</sup> from the theory of Lifshitz<sup>12</sup> is for the present system

$$V(R) = -k_L / R^3, \quad (4)$$

where

$$k_L = \frac{\kappa T}{2} \sum_{n=0}^{\infty} \alpha(i\xi_n) \frac{\epsilon(i\xi_n) - 1}{\epsilon(i\xi_n) + 1} (1 + r_n + \frac{1}{4} r_n^2) e^{-r_n}, \quad (5)$$

where  $\xi_n = (2\kappa T / \hbar)n$ ;  $\kappa$  is Boltzmann's constant;  $r_n = 2\xi_n R / c$ ;  $c$  is the speed of light;  $\alpha(i\xi_n)$  and  $\epsilon(i\xi_n)$  are respectively the polarizability of the atom and the dielectric susceptibility of the metal evaluated on the imaginary frequency axis; the prime on the summation indicates that the  $n=0$  term be multiplied by  $\frac{1}{2}$ . In this expression, one ignores the fact that the susceptibility  $\epsilon(i\xi)$  of the gold should represent a nonlocal response. This limitation has been examined for metallic conductors by Chang *et al.*<sup>21</sup> via a hydrodynamic model for conduction electrons. They concluded that the Lifshitz theory as employed below agrees with their result which is valid to lowest orders in the spatial variation of the dielectric response. The numerical importance of discrepancies in higher orders is still undetermined.

TABLE VI. Comparison of predicted and measured interaction constants.

	Cs	Rb	K
Lennard-Jones, Eq. (1)	40.1	29.4	23.2
Bardeen, Eq. (2)	30.1	21.6	16.9
Mavroyannis, Eq. (3)	26.2	19.8	16.4
Parsegian, Eq. (5)	11.4	9.70	8.94
Observed	$7.00 \pm 0.29$	$6.04 \pm 0.30$	$5.10 \pm 0.62$

TABLE VII. Comparison of two different sets of wave functions for computing the interaction constant of potassium with a conducting surface.

	NS =	Cross integrals					
		1S	2S	3S	4S		
$\langle 3P r nS \rangle$	Clementi	0.0590489	0.359367	0.0922987	0.0141222		
	Froese	0.059050	-0.359377	0.092284	0.015033		
$\langle 3P r nS \rangle$	Clementi	-0.0150372	0.101899	1.32897	0.450714		
	Froese	0.015025	0.101896	1.329038	0.462469		
Direct integrals							
	$\langle 1S r^2 1S \rangle$	$\langle 2S r^2 2S \rangle$	$\langle 3S r^2 3S \rangle$	$\langle 4S r^2 4S \rangle$	$\langle 2P r^2 2P \rangle$	$\langle 3P r^2 3P \rangle$	
Clementi	0.0089135	0.176593	1.88327	31.5206	0.150787	2.43985	
Froese	0.008913	0.176592	1.883448	31.544353	0.150801	2.440655	

The coefficient  $k_L$  in Eq. (5) is a sum of terms, each with a different  $R$  dependence, for different eigenfrequencies  $\xi_n$  as summarized in the ratio  $\gamma_n$ . The potential  $V$  is thus not strictly inverse cube in  $R$ . At very small separations such that all  $\gamma_n$  are effectively zero,  $k_L$  is constant and  $V$  goes as  $R^{-3}$ . At very large separations, all  $\gamma_n$  are much greater than 1, except  $\gamma_0$  which is always zero; one term then remains in the sum, and the potential is again  $R^{-3}$ . In between, there is no simple power law, but for a small range  $k_L$  goes as  $R^{-1}$  and the potential is inverse fourth power in  $R$ . This will be illustrated in Fig. 5 below.

The atomic polarizability can be calculated by the familiar expression:

$$\alpha(\omega) = \sum_i \frac{e^2}{m} f_{0i} (\omega_i^2 - \omega^2)^{-1}, \quad (6)$$

where  $m$  is the electron mass,  $f_{0i}$  is the oscillator strength of the  $i$ th excited-state-to-ground-state transition, which is tabulated by Norcross<sup>22</sup> for Cs, Weisheit<sup>23</sup> for Rb, and by Wiese *et al.*<sup>24</sup> for K.

Johnson and Christy<sup>25</sup> have measured optical constants for gold, and found that the dielectric constant of gold follows the Drude free-electron theory

$$\epsilon(\omega) = 1 - \frac{\omega_p^2}{\omega(\omega + i/\tau)}, \quad (7)$$

where for gold  $\hbar\omega_p = 9$  eV and  $\tau = 9.3 \times 10^{-15}$  sec.

As mentioned above,  $k_L$  is not really a constant. Because of the finite velocity of light,  $k_L$  decreases as the separation between atom and surface increases. This is referred to as the "retardation effect." With the help of Eqs. (6) and (7), we have evaluated  $k_L$  between a Cs atom and a gold surface for an extended range of  $R$ , and the result is plotted in Fig. 5. Clearly, below  $\sim 200$  Å,  $k_L$  remains constant (thus, the potential is truly  $R^{-3}$ ); above  $\sim 5000$  Å, the potential approaches an  $R^{-4}$  form as demonstrated by the  $-1$  slope of  $k_L$ .

Cs atoms deflected into the region of interest have impact parameters between 500 and 800 Å (see Table VIII). In this region, the Lifshitz potential shows a slight deviation from the  $R^{-3}$  potential (see Fig. 5). For example, at  $R = 500$  Å,  $k_L = 11.4 D^2$ , and at  $R = 600$  Å,  $k_L = 10.9 D^2$ , a 5% decrease. This deviation is not strong enough to conflict with our observation which indicates the consistency with an  $R^{-3}$  potential. The measurement is probably not precise enough to reveal such a small change in the functional form.

Along the trajectory of an atom, the separation between the atom and the surface varies from the minimum approach  $\lambda$  (slightly smaller than the impact parameter) to practically infinite distance. The discrepancy between the theory and the observation might conceivably arise from this neglect of the retardation effect in the path integration. We do not expect this to be so, because during the time that the atom is far away from the surface, the interaction does not contribute significantly to the deflection of the atom. Indeed, a calculation shows that about 90% of the impulse is applied to the atom while the atom is within a distance of the impact parameter plus 200 Å from the surface. In fact, we have generated a beam profile for a Cs beam and a gold surface using the full Lifshitz

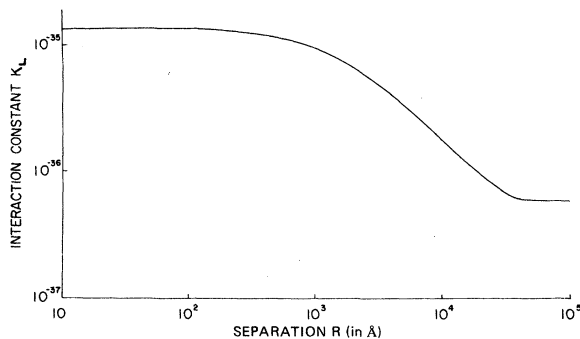


FIG. 5.  $k_L$  is plotted as a function of the separation  $R$ .

TABLE VIII. Predicted relation between observed Cs beam deflection  $S$  and impact parameter  $A$ . For a set of deflected distances  $S$ , the corresponding impact parameter is calculated assuming  $V(R) = k/R^3$  with  $k = 7.0 D^2$ , and temperature of the beam 385 °K.

Deflection distance	$S$ (cm)	0.01	0.03	0.05	0.07	0.10	0.12	0.14
Impact parameter	$A$ (Å)	785	605	551	526	508	502	498

potential form in Eq. (5), and found that the calculated beam profile is still significantly larger than the observed profile (see Fig. 6).

We further compare the predicted interaction strengths with the observed values. The  $k_L$  listed in Table VI are evaluated at  $R = 500$  Å. These values are a factor  $\sim 1.6$  larger than the observed values. Nevertheless, among the theoretical values they are the closest to those inferred from measurement.

#### DISCUSSION

It is not surprising that the prediction based on the Lifshitz theory<sup>8,12</sup> is closer to the observation than those by Lennard-Jones,<sup>1</sup> Bardeen,<sup>2</sup> and Mavroyannis<sup>5</sup> based on the image model. The model of Parsegian using the Lifshitz theory is, on the other hand, neither an image nor a London picture: it is impossible to speak of interaction with a gold conductor as a pairwise-sum interaction, because the conducting electrons are not localized. This freedom is an integral part of the

generalized theory of Van der Waals forces by Dzyaloshinskii, Lifshitz, and Pitaevskii<sup>12</sup> (DLP). In this approach, the interaction is treated as being established through a fluctuating electromagnetic field. No particular model of the molecular structure of the atom or the metal is assumed, and the two quantities, the dielectric susceptibility of the metal and the polarizability of the atom, determine the interaction energy completely.

The success of the DLP approach has been demonstrated experimentally in many applications.<sup>26-29</sup> However, its validity has not been confirmed in the interaction between an atom and a surface.

Even though the Lifshitz prediction is closest to our result, the discrepancy is significant:  $k_L$  is larger than our observation by about 60%, while the uncertainty of the measurement is claimed to be about 5-10%.

Surface contamination and surface roughness are two possible sources of discrepancy:

(1) Surface contamination: Schrader<sup>30</sup> has argued convincingly that the tendency of gold surfaces to attract hydrocarbon contaminants can cause serious errors in measured wettability. We have taken special precaution to avoid such contamination. No mechanical or diffusion vacuum pump has been used at any time. Still, the surfaces are not atomically clean even inside the ultrahigh vacuum used here.

As a control, we have made a clear surface by vacuum deposit *in situ*. Gold wires were wrapped around a tungsten heater 8 in. away from the substrate (see Fig. 1). A shutter placed between the evaporator and the surface was lifted up only during the deposition, and a Sloan Quartz crystal oscillator is used to monitor the deposition. During the deposition, the pressure in the chamber rises to about  $4 \times 10^{-10}$  Torr, and within a minute after the completion of the deposition, the pressure falls below  $1 \times 10^{-10}$  Torr.

It takes about ten minutes to reach the base pressure. For a clean surface exposed to a vacuum of  $10^{-10}$  Torr, it takes more than  $10^4$  sec (3 h) to form a monolayer of gases on the surface. Thus, we have an atomically clean surface for sufficient time to perform measurements. With a clean surface prepared this way, the measurement shows no appreciable difference from

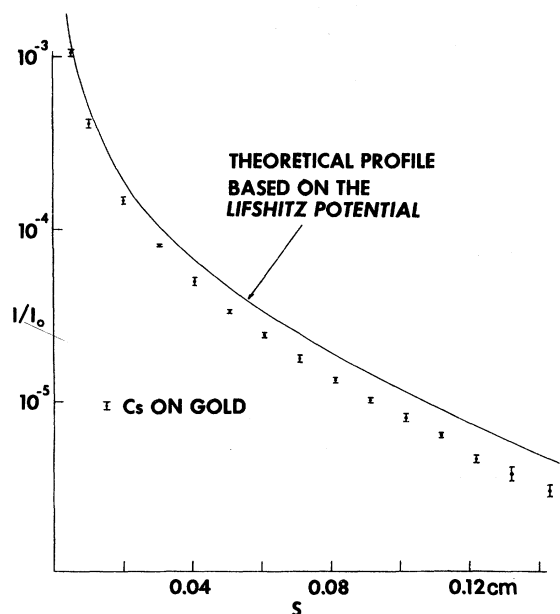


FIG. 6. Observed profile of Cs on Au is compared with the profile calculated using the full expression of the Lifshitz potential [i.e., Eqs. (4) and (5)].

the result of other gold surfaces.

(2) Surface roughness: The substrates of the evaporated gold surface are a stainless-steel cylinder polished to 1/20 of wavelength (250 Å) and ordinary drawn-glass tubing. We have not measured surface topography of the gold-coated surfaces. Neither do we have a workable theoretical model to study the effect of the surface roughness. Nevertheless, we do not expect that the interaction is affected by the surface roughness of such small magnitude as present on the surface. The good internal consistency of our data suggests that surface roughness is not a major effect. The substrates of the two gold surfaces are quite dif-

ferent in terms of surface topographies, yet the beam profiles of those two surfaces agree well with each other<sup>11</sup>; even the difference between the profiles of the gold surfaces and the stainless-steel surface is very small.<sup>11</sup>

We intend to carry out a better test on the effect of roughness by obtaining data with an atomically smooth surface. A slice of cleaved mica may be stuck onto a cylindrical surface to make a substrate which is believed to be atomically smooth<sup>26,29</sup>; or liquid metals such as indium, gallium, or thallium may be set in a container whose walls are not wetted by the liquid metal, to create a positive meniscus.

---

\*Present address: Code 5230, Surface Physics Branch, Naval Research Laboratory, Washington, D.C. 20375.

- <sup>1</sup>J. E. Lennard-Jones, *Trans. Faraday Soc.* **28**, 334 (1932).
- <sup>2</sup>J. Bardeen, *Phys. Rev.* **58**, 727 (1940).
- <sup>3</sup>H. Margenau and W. G. Pollard, *Phys. Rev.* **60**, 128 (1941).
- <sup>4</sup>H. B. C. Casimir and D. Polder, *Phys. Rev.* **73**, 360 (1948).
- <sup>5</sup>C. Mavroyannis, *Mol. Phys.* **6**, 593 (1963).
- <sup>6</sup>A. D. McLachlan, *Proc. R. Soc. A* **271**, 387 (1963).
- <sup>7</sup>T. H. Boyer, *Phys. Rev. A* **5**, 1799 (1972); **6**, 314 (1972); **7**, 1832 (1973).
- <sup>8</sup>V. A. Parsegian, *Mol. Phys.* **27**, 1503 (1974).
- <sup>9</sup>E. J. R. Prosen and R. G. Sachs, *Phys. Rev.* **61**, 65 (1942).
- <sup>10</sup>A. Shih, D. Raskin, and P. Kusch, *Phys. Rev. A* **9**, 652 (1974).
- <sup>11</sup>A. Shih, *Phys. Rev. A* **9**, 1507 (1974).
- <sup>12</sup>E. M. Lifshitz, *Zh. Eksp. Teor. Fiz.* **29**, 94 (1955) [*Sov. Phys.—JETP* **2**, 73 (1956)]; I. E. Dzyaloshinskii, E. M. Lifshitz, and L. P. Pitaevskii, *Adv. Phys.* **10**, 165 (1961).
- <sup>13</sup>Paul G. Hoel, *Introduction to Mathematical Statistics*, 3rd ed. (Wiley, New York, 1965), p. 134.
- <sup>14</sup>*Mathematical Tables from Handbook of Chemistry and Physics* (Chemical Rubber Co., Cleveland, 1953), p. 283.
- <sup>15</sup>Harry H. Ku, in *Handbook of Industrial Metrology* (Prentice-Hall, New York, 1967), p. 31.
- <sup>16</sup>C. Froese Fischer and M. Wilson, Programs for Atomic-Structure Calculations, Argonne National Laboratory, Report No. ANL-7404 (unpublished).
- <sup>17</sup>D. Pines, in *Solid State Physics*, edited by F. Seitz and D. Turnbull (Academic, New York, 1955), Vol. 1.
- <sup>18</sup>C. E. Moore, *Atomic Energy Levels*, Natl. Bur. Stds., Circ. No. 467 (U.S. GPO, Washington, D.C., 1958).
- <sup>19</sup>R. Wolof, H. Schwartz, T. Miller, B. Bederson, and J. Park, *Bull. Am. Phys. Soc.* **18**, 1500 (1973).
- <sup>20</sup>Enrico Clementi, *Tables of Atomic Functions* (IBM, 1965).
- <sup>21</sup>D. B. Chang, R. L. Cooper, J. E. Drummond, and A. C. Young, *J. Chem. Phys.* **59**, 1232 (1973).
- <sup>22</sup>David W. Norcross, *Phys. Rev. A* **7**, 606 (1973).
- <sup>23</sup>J. C. Weisheit, *Phys. Rev. A* **5**, 1621 (1972).
- <sup>24</sup>W. L. Wiese, M. W. Smith, and B. M. Glennon, *Atomic Transition Probabilities*, NSRDS-NBS 4 (U.S. GPO, Washington, D.C., 1969), Vol. II.
- <sup>25</sup>P. B. Johnson and R. W. Christy, *Phys. Rev. B* **6**, 4370 (1972).
- <sup>26</sup>J. N. Israelachvili and D. Tabor, *Proc. R. Soc. A* **331**, 19 (1972); *Prog. Surf. Memb. Sci.* **7**, 1 (1973); P. Richmond and B. W. Ninham, *J. Colloid Interface Sci.* **40**, 406 (1972).
- <sup>27</sup>E. S. Sabisky and C. H. Anderson, *Phys. Rev. A* **7**, 790 (1973).
- <sup>28</sup>D. Gingell and V. A. Parsegian, *J. Theor. Biol.* **36**, 41 (1972).
- <sup>29</sup>D. Tabor and R. H. S. Winterton, *Proc. R. Soc. A* **312**, 435 (1969).
- <sup>30</sup>M. E. Schrader, *J. Phys. Chem.* **74**, 2313 (1970).